Design Optimisation of an Electrostatic MEMS Actuator with Low Spring Constant for an "Atom Chip"

H.A. Rouabah, C.O. Gollasch and M. Kraft

University of Southampton, School of Electronics and Computer Science,
Highfield, Southampton, SO17 1BJ, UK.
(har04r , cg102r, mk1)@ecs.soton.ac.uk

ABSTRACT

A new spring shape is designed for a MEMS three dimensional electrostatic actuator. A low spring constant in Z direction for a thick structural layer is achieved. Characteristic features and challenges of this design are described and the analytical analysis is verified by FEM simulations using CoventorWare™. The analytical models are derived for two types of serpentine springs namely a square serpentine spring (SSS) and curved serpentine spring (CSS). The analytical results are in very good agreement with the simulations.

Keywords: MEMS, electrostatic suspension, spring constant, actuator, modelling

1 INTRODUCTION

The use and application of MEMS based sensors and actuators have had a significant impact in the engineering industry during the last decade. These devices also show promise for a variety of future applications which are currently the subject of research worldwide. One of such applications is the so-called atom chip [1], [2], where a cloud of ultra cold atoms in a Bose Einstein Condensate (BEC) is controlled and manipulated by magnetic confinement fields [3], [4]. These atom chips comprise a range of microfabricated devices such thick gold wires, mirrors for optical cavities and a three dimensional (3D) electrostatic actuator [5], [6]. The latter is an important part of the atom chip and allows the precise spatial alignment between an optical fibre and a mirror, forming an optical cavity. This cavity is used to detect the BEC atom cloud. The design and fabrication of such an electrostatic 3D actuator is the most challenging part from the micromachining point of view.

An earlier study has looked at the XY motion for the in-plane positioning of an optical cavity opposite an optical fiber [7], [8]. The XY actuator uses conventional comb drives to achieve a motion envelope of approximately ±11µm for a voltage of 115V.

To provide actuation in the third dimension (i.e. in the Z direction), a parallel plate electrostatic actuator is required. The function of the electrostatic actuator is based on both electrostatic and mechanical forces that are generated by two capacitor plates and a suspension system, respectively.

For the comb drives of the in-plane XY-actuator a thick structural layer is desirable. However, this leads to a high spring constant in the Z direction and hence requires a high actuation voltage. Our fabrication process uses a 60 µm thick structural layer. In a previous design we used a square serpentine spring (SSS) which has been employed for similar MEMS actuators in the Z direction [9],[10]. Its advantages are a relatively low spring constant in a compact area as well as providing low cross-axis sensitivity motion in the vertical and lateral directions. For the SSS design, the actuation voltage are still relatively high, therefore we are proposing a new shape of suspension system that fits in a circular area. It is based on a curved serpentine spring (CSS) and is shown in Figure 1. Using a circular shape allows the central platform that is being moved to be attached to the substrate with only three springs, whereas a square design required four separate springs.

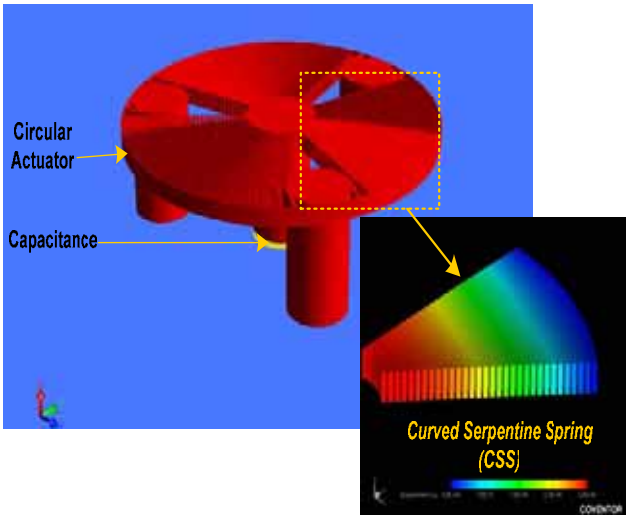

Figure 1: The circular actuator model with curved serpentine spring (CSS)

For design optimization an analytical model, especially of the spring constant, is of crucial importance. In the next sections the derivation of a semi-analytical modelling approach is presented, followed by a comparison between the two suspension systems (CSS and SSS) and verification of the analytical models by FEM simulation using CoventorWare™ software.

2 THEORETICAL ANALYSIS

Since both springs SSS and CSS behave in a similar manner, the analytical model of the SSS is derived first as its structure is simpler, and then the CSS analytical model is deduced.

2.1 SSS Modelling

The SSS is folded in regular equal segments that compose of many L-shape meanders connected to each other (see Fig.2).

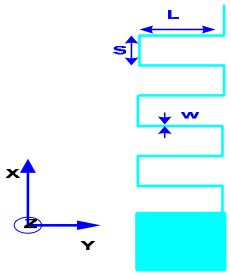

Figure 2: The squared serpentine spring (SSS) design indicating the relevant geometrical parameters.

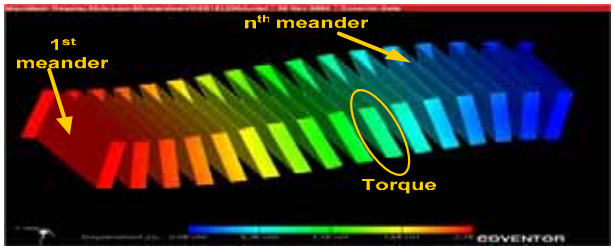

Figure 3: CoventorWare™ model of the (SSS) structure.

The total spring constant is a combination of the bending stiffness of all beams. The spring constant for a single L shape meander is derived first, and then it will be generalized for N meanders.

For this analysis it is assumed that any beam displacements are due to bending and torsion. Other effects such as deformations from shear, compression and traction are neglected. This is a valid assumption for small deflections.

The spring constant in Z direction for the first L-shape meander has a contribution from the long and the short beam. The stiffness of the long beam segment is given by [11]:

$$K_A = \frac{3EI}{L^3} \tag{1}$$

where L is the length of the longer beam, E is Young modulus (E=169GP) and I the bending moment of inertia for a rectangular beam.

The stiffness of the shorter beam, K_B, can be derived by applying a force F at the end of the long beam which creates a torsion T on the short beam leading to a deflection of the long beam. Assuming a small deflection angle θ and dividing the torsion T by θ gives:

$$\frac{T}{\theta} = K_B L^2 \tag{2}$$

On the other hand, the governing equation for tensional structures deflecting through an angle is [12]:

$$\frac{T}{\theta} = \frac{hG}{s} \tag{3}$$

with G being the shear modulus of elasticity for isotropic materials:

$$G = \frac{1}{2(1+\nu)} \tag{4}$$

and h is a constant depending on the geometry of the beam which is given for the rectangular L-shape beam by [13]:

$$h = tw^3\left[\frac{1}{3} - 0.21\frac{w}{t}\left(1 - \frac{w^4}{12t^4}\right)\right] \tag{5}$$

where s is the length of the shorter beam, w the width of the spring, t the thickness of the spring and ν Poisson's ratio for silicon (ν=0.3).
Using equations (2) and (3) and solving for K_B gives:

$$K_B = \frac{hG}{s.L^2} \tag{6}$$

The total spring constant for one L-shape segment is therefore given by [14]:

$$\frac{1}{K_z} = \frac{1}{K_A} + \frac{1}{K_B} \tag{7}$$

Substituting the expressions for K_A and K_B into equation (7) results:

$$K_z = \frac{hG}{L^2\left(\frac{hG}{EI}L + 3s\right)} \tag{8}$$

Equation (8) represents the spring constant of only the first L-shape meander. However, the stiffness of the n^{th} meander segment of the spring differs from the first

meander segment. To generalize the equation of the spring constant for the n[th] meander, we assume that there exists a function f_n^{sss} which depends on the number of meanders N, lengths L and s, width w, and thickness t. Therefore, the spring constant for the n[th] meander K_{Z_n} is given by:

$$K_{Z_n} = K_1 f_n^{sss}(L, s, w, t) \tag{9}$$

K_1 is the spring constant of the first meander taken from equation (8). The total spring constant in Z direction K_Z^{sss}, of the SSS suspension design for N meanders is then given by:

$$\frac{1}{K_Z^{sss}} = \sum_{n=1}^{N} \frac{1}{K_{Z_n}} \tag{10}$$

As K_1 is constant, the sum given in equation (10) becomes:

$$\frac{1}{K_Z^{sss}} = \frac{1}{K_1} \sum_{n=1}^{N} \frac{1}{f_n^{sss}} \tag{11}$$

The sum $\sum_{n=1}^{N} \frac{1}{f_n^{sss}}$ can be abbreviated by a new function α that depends on the same variables L, s, w, t and N. Using dimensional analysis, the function α can be written as following:

$$\alpha \propto L^a . s^b . w^c . t^d . N^e \tag{12}$$

The coefficients a, b, c, d and e represent the power of each variable. These coefficients are determined numerically from FEM simulation. For our problem α was found to be:

$$\alpha = \frac{720}{N^3} \sqrt{\frac{L\,t}{\sqrt{s}\;w}} \tag{13}$$

Using equations (8) and (13) in (11), the final equation for the Z-direction spring constant is:

$$K_Z^{sss} = \frac{720}{N^3} \cdot \sqrt{\frac{L\,t}{\sqrt{s}\;w}} \cdot \frac{hG}{L^2\left(\frac{hG}{EI} L + 3s\right)} \tag{14}$$

2.2 CSS Modelling

The CSS is characterised by a regular augmentation in the long beam L_n and is a function of both the angle β and the number of meanders N. Figure 4 shows the new suspension system with all relevant parameters.

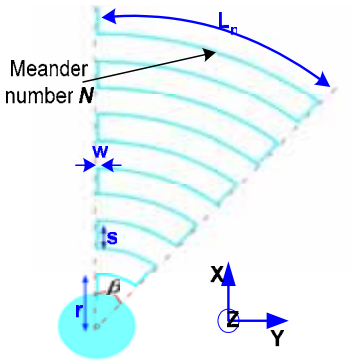

Figure 4: Geometrical parameters used for the derivation of the curved serpentine spring (CSS) design.

The length L_n is given by:

$$L_n = \beta(n(w+s)+r) \tag{15}$$

where β is the opening angle of the spring, n refers to the n[th] meander, w the width of the meander, s the length of the short beam and r the initial radius of the first curved segment. In an analogous way to the SSS design analysis, the spring stiffness of the n[th] meander is given by:

$$K_{Z_n} = K_1 f_n^{css}(L_n, s, w, t) \tag{16}$$

In contrary to the SSS design analysis a function f_n^{css} has to be found for each spring meander instead of a function for the sum over all meanders. This is because L_n varies from meander to meander and hence a FEM simulation has to be run for each meander. From FEM simulations a function f_n^{css} can be found for the n[th] meander:

$$f_n^{css} = \frac{1}{60n} \sqrt{\frac{L_n\,t}{nw\sqrt{s}}} \tag{17}$$

If the curved meanders are approximated by straight lines, equation (8) can be used to describe the spring constant of the first meander. Thus, by combining equations (8) and (17) the overall spring constant is given:

$$K_Z^{css} = \left[\sum_{n=1}^{N} 60n \sqrt{\frac{nw\sqrt{s}}{L_n t}} \cdot \frac{L_n^2}{Gh}\left[\left(\frac{Gh}{EI}\right) L_n + 3s\right]\right]^{-1} \tag{18}$$

3 SIMULATION RESULTS

Assuming the same area for CSS and SSS suspension design, the spring constant in Z direction, which defines the mechanical reaction force, has been reduced by approximately a factor of three. This leads to a nine times a

lower actuation voltage since the electrostatic force is proportional the voltage squared. A further reduction is expected as only three meander springs are required, as compared to four for a SSS spring design.

To validate the analysis, FEM simulations using CoventorWare™ were carried out. As expected, for the same displacement the required force for a CSS design is about three times less than a SSS design. The results are shown in Figure 5. Furthermore, the range in which the suspension system behaves like a linear spring has been expanded.

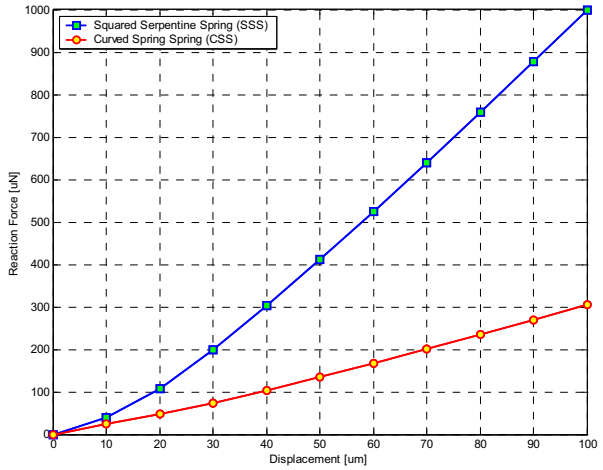

Figure 5: FEM simulations of the reaction force as a function of displacement for SSS and CSS suspension systems.

Figure 6 shows a comparison between FEM simulation results and the derived analytical model. The agreement is within 10%; for small displacements it is even significantly better.

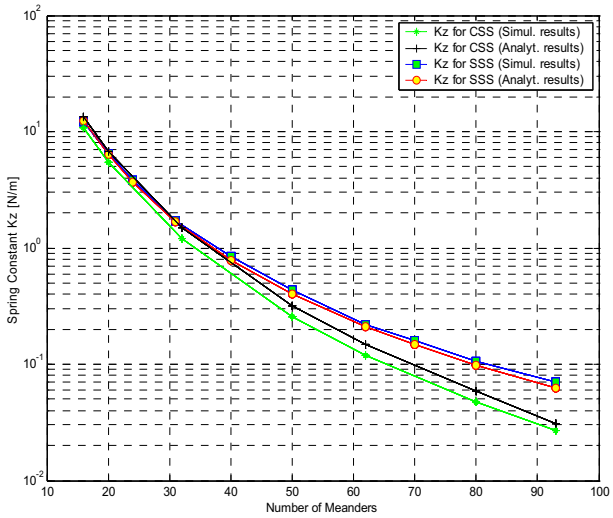

Figure 6: Comparison between the simulated and analytical models of the spring constants in Z direction for both spring designs.

4 CONCLUSION

This paper shows how the application of a novel suspension has led to an improvement in the design performance in the Z direction of a 3D electrostatic actuator for an atom chip. The design has achieved a lower spring constant in Z direction, and hence a reduced actuation voltage requirement. The analytical models derived are in a good agreement with FEM simulations.

ACKNOWLEDGEMENTS

The author owes extreme gratitude to Dr. Joost van Kuijk, CoventorWare European technical director, for his remarkable technical skills and invaluable help and suggestions.

REFERENCES

[1] R. Folman, et. al. Phys. Rev. Lett., 84, 4749-4752, 2000.
[2] M. Bartenstein, et. al. IEEE Journal of Quantum Electronics, 36 , 1364 – 1377, 2000.
[3] S. Du, et. al., Phys. Rev.A, 70 , 053606, 2004.
[4] A. Kasperet. al. J. of Optics B: Quantum and Semiclassical Optics, 5, S143–S148, 2003.
[5] Z. Moktadir, et. al., J. Micomech. Microeng., 14, 82-85, 2004.
[6] E. Koukharenko, et, al. , Sensors and Actuators, A 115, 600–607, 2004.
[7] C. O. Gollasch, et. al., In Proc. of 15th MicroMechanics Europe Workshop, 33-36, 2004.
[8] C. O. Gollasch, et. al., In Proc. of Eurosensors XVIII, 2004.
[9] S. Pacheco, C.T.C. Nguyen and L.P.B. Katehi, IEEE MTT-S Digest., 3 , 1569 – 1572, 1998.
[10] S.P. Pacheco, L.P.B. Katehi, C.T.C. Nguyen, IEEE MTT-S Digest. 1, 165–168, 2000.
[11] J. K.Yee, "Shock Resistance of Ferromagnetic Micromechanical Magnetometers," MSc Thesis, University Of California Los Angeles, 16-17, 2003.
[12] Gregory T.A. Kovacs, "Micromachined Transducers Sourcebook," McGraw-Hill, 183,187, 1998.
[13] Roark Raymond and J. Raymond, "Roark's formulas for stress and strain," McGraw-Hill, 1989.
[14] Joseph Shigley, "Mechanical engineering design," McGraw-Hill, 91, 1972.